

**Evaluate Infill Drilling Options in Hugoton Field  
– Nine Section Area around Flower A1 well**

**KGS OFR 2009-8**

**Saibal Bhattacharya**

## **Introduction**

The goal of this study was to simulate a) the expected production from an infill well(s) like the Flower A1 (and possible 4<sup>th</sup> well per section) under different completion scenarios such as vertical and horizontal, and b) to understand the interference on production from existing (vertical) wells as a result of the completion of an additional infill well (4<sup>th</sup> well) in each section. A 9-section area around the Flower A1 well was selected because a reservoir model had been developed for this area (Figure 1) as a part of a previous study (Bhattacharya, et. al, 2005), and this model served as a basis to history match production and available pressure data (including limited layer pressures) over a period extending from start of production in 1938 to July 2003.

### **Modeling of Hydraulic Fracturing**

Independent of this study, hydraulic fracture characterization was carried on by integrating the Flower area reservoir model, available rock-mechanics data, simulator-calculated layer pressures (at select times), and data from operators regarding prevalent hydraulic fracturing operations. These studies helped to model the way a fracture would most likely propagate in the Hugoton field in the vicinity of the Flower A1 well given the prevalent fracturing parameters. Based on the results of the fracture simulation studies, it was decided that the most probable fracture characteristics for a vertical infill well (such as the Flower A1 to be completed as of January 1 2008) to be described as input to the reservoir simulator would be as follows:

- a) fracture extending vertically from Herrington (Layer 1) to B4\_Lime (Layer 21),
- b) fracture permeability taking values such as 4000 md, 8000 md, and 11,000 md, and
- c) fracture half-length taking values such as 162 ft and 325 ft.

When completing the Flower A1 as a horizontal well (as of January 1 2008) in the reservoir simulator, the most probable fracture characteristics identified for this study included:

- a) stratigraphic placement of the horizontal well in Lower Fort Riley (Layer 9),
- b) fracture extending vertically from Krider (Layer 2) to A1\_LM (Layer 13),
- c) fracture permeability taking values such as 8000 md and 11,000 md, and
- d) fracture length (from heel to toe) of 1500 ft.

Two scenarios were modeled when the Flower A1 was completed as a horizontal infill well in this study:

- a) as a horizontal infill well with a lateral fracture along its entire length, and
- b) as a horizontal infill well with transverse fractures (each 1500 ft long) that were perpendicular to the length of the horizontal lateral.

## Vertical Infill Wells – Fracture Half-lengths & Permeability

Figures 2A to 2C show the location of the Flower A1 (Flwr) in the study area and the distribution of refined grids used to define the east-west trending hydraulic fracture at the well. Refined grids cells of 8.8 ft by 1 ft (Figure 2C) were used to define the east-west trending hydraulic fracture at the Flower well. The permeability (in lateral and vertical directions) for the grids defining the hydraulic fracture was set to values such as 4000 md, 8000 md, and 11,000 md, respectively for each model. Linear relative permeability curves (for gas and water) were assigned to these (refined) grids that defined the fracture.

Figure 3 summarizes the results obtained from simulations where the Flower A1 well was completed as of 1/1/2008 as a vertical well that was hydraulically fractured. Modeled fracture half-length ( $H_f$ ) was assumed to be 325 ft and fracture permeability ( $K_f$ ) was varied from 4000 md to 11,000 md. Two sets of simulations were carried out using the previously mentioned settings with the BHFP (bottom hole flowing pressure,  $P_{wf}$ ) being set to 14.7 psi in one set (broken lines) and to 28 psi in the other set (unbroken lines). The plotted annual average production rates were calculated by dividing simulator-calculated annual cumulative volumes by 365 days for every year from 2008 to 2028.

At a constant BHFP ( $P_{wf} = 14.7$  or  $P_{wf} = 28$  psi), the simulator-calculated (gas) production rates varied little above  $K_f = 8000$  md. However, for a constant fracture permeability (such as  $K_f = 11,000$  md), the gas flow rates varied significantly when  $P_{wf}$  was changed from 28 psi to 14.7 psi, such as from 130 mcf/d (average 1<sup>st</sup> year) at  $P_{wf} = 28$  psi to 195 mcf/d (average 1<sup>st</sup> year) at  $P_{wf} = 14.7$  psi. This difference in annual rates prevailed over the succeeding years in the modeled 20-year well life resulting in a difference in the cumulative gas production from 0.31 bcf ( $P_{wf} = 28$  psi) to 0.689 bcf ( $P_{wf} = 14.7$  psi). Attaining high fracture permeability ( $K_f \geq 8000$  md) is one of the goals for any designed hydraulic fracture job. However, it should be noted that above a certain fracture permeability ( $K_f \geq 8000$  md), the incremental production from the reservoir appears to be limited by its deliverability, and thus achieving higher  $K_f$  would not net any significant additional volumes of gas. It is apparent from these results that the operator should make all attempts to flow these wells with minimal or no fluid columns, because both flow rates and cumulative production is significantly affected by the back pressure exerted by as small as 30 ft of fluid column in the well.

Figure 4 plots the production from the Flower A1 well when completed as hydraulically fractured with  $H_f = 165$  ft. By halving the  $H_f$  from 325 ft to 162 ft, cumulative production (over a 20-yr period) declined from 0.31 bcf to 0.255 bcf (for  $K_f = 11,000$  md and at  $P_{wf} = 28$  psi), and from 0.689 bcf to 0.549 bcf (for  $K_f = 11,000$  md and at  $P_{wf} = 14.7$  psi), respectively. Minor amounts of back-pressure (i.e., higher  $P_{wf}$ ) affect the simulator-calculated Flower infill well production rate more adversely than shorter fracture half-lengths. Thus from the operator's standpoint, the critical factor to maximize production from an infill well such as the Flower A1 will be to produce the well against minimum or no fluid column. Secondly, hydraulic fracturing should be designed to result in a fracture with the maximum  $H_f$  and modest  $K_f$  (conductivity).

## Contribution of Tight Zones

Figure 5 plots the simulator-calculated volume of remaining gas in each layer as gas flows in and out of each layer through time (i.e., from 1938 to 2028) in the 9-section area around the Flower A1 (vertical) well, which starts to produce (at  $P_{wf} = 14.7$  psi) as of 1/1/2008 (till 1/1/2028) in the simulator and where the hydraulic fracture is defined by  $H_f = 325$  ft and  $K_f = 11,000$  md. Gas volumes moving out of each layer may get produced at the neighboring wells and/or may travel into adjacent layers. Assuming that most of the gas leaving a layer flows into a neighboring well and following the rate of decline of the remaining-gas curves, it appears that Krider was the dominant contributor to gas production till 1980. Thereafter, volumes of gas flowing out of Towanda and Fort Riley zones started to exceed that from Krider, and this dominance of Towanda and Fort Riley zones continued to the end of the period simulated (i.e., 2028).

Figure 6 plots the percentage contribution of each major layer to the total gas moving out of all the above stated layers in the post-2008 period. It is evident that Towanda and Fort Riley contributed around 25% (each) while Wreford showed increasing contribution varying from 12% to 17% over the time period plotted. Contribution from the Lower Fort Riley is about 10% while that from Winfield varied from 11% to 8% over the same period of time. Interestingly, the contribution of Krider declined from around 10% to 2% over this same time. Thus, the post-2008 production is dominated by gas moving out of tighter layers such as Towanda (Flower DST permeability = 1.2 md), Fort Riley (Flower DST permeability = 0.43 md), Wreford (Flower DST permeability = 0.5 md), and Lower Fort Riley (Flower upscaled permeability = 0.02 md), which together contributed about 75% of the total gas volumes flowing out of all the layers shown in the plot.

## Horizontal Infill Wells – Fractured Laterally

Simulation studies were carried out by completing the Flower A1 (Flwr) well as a horizontal well 1500 ft long and hydraulically fractured along its lateral length. Figures 7A to 7C show the location of the Flower horizontal well among existing Chase and Council Grove wells, and the refined grids used to define the high permeability (11,000 md shown in red grid cells) existing in the hydraulic fracture.

Results plotted in Figure 8 compare the simulator-calculated production from the Flower horizontal well assuming  $K_f = 11,000$  md and  $K_f = 8000$  md in the lateral fracture system established along the length of the well. It is apparent from the above figure that fracture conductivity in the horizontal well does not matter as long as a reasonable conductivity (around 8000 md) has been established during fracturing and stimulation process. Figure 8 also compares the anticipated production from a Flower horizontal well that is laterally fractured along the well length with that from Flower when completed as a vertically fractured well. Assuming  $K_f = 11,000$  md, the horizontal well recovers 1.3 times as much gas (0.913 bcf as compared to 0.689 bcf) as a vertical well hydraulically fractured with  $H_f = 325$  ft, and 1.7 times as much gas (0.913 bcf as compared to 0.549 bcf) as a vertical well hydraulically fractured with  $H_f = 162$  ft. Thus under the conditions simulated, the production from the Flower well completed horizontally and laterally fractured exceeds

that from the same well completed vertically and hydraulically fractured by no greater than 1.7 times, and this is a critical input while evaluating the economic viability of completing infill wells in the Hugoton field as laterally fractured horizontal wells.

### **Horizontal Infill Wells – Fractured Transversely**

The Flower A1 well (Flwr) was also modeled as a horizontal well of 1500 ft lateral length that was intersected by three transverse fractures at the heel, toe, and mid-section. Each transverse fracture was assumed to have  $H_f = 750$  ft. Two scenarios, one with  $K_f = 11,000$  md and another with  $K_f = 8000$  md, were simulated. Figure 9A shows the location of the Flower horizontal well with transverse fractures, while Figure 9B shows the distribution of refined grids to model the fractures. Figure 9C shows the presence of high permeability ( $K_f = 11,000$  md marked by grid cells in red) in the transverse fracture passing through the heel of the well.

Figure 10 plots the simulator-calculated average annual production from Flower horizontal well with a lateral length of 1500 ft and completed with one, two, or three transverse fractures each with  $H_f = 750$  and  $K_f = 11,000$  md. This plot also compares these rates against those calculated for Flower horizontal well that was hydraulically fractured along its lateral length of 1500 ft and with  $K_f = 11,000$  md. It is apparent from this plot that the horizontal Flower well fractured along its lateral length produces 1.15 times more gas (0.913 bcf vs. 0.795 bcf) as a horizontal Flower well completed with three equidistant transverse fractures along its length. The Flower horizontal well, when completed with a single transverse fracture (at the toe), has a cumulative production of 0.382 bcf while a comparable vertical Flower well with  $H_f = 162$  ft is estimated to produce 0.524 bcf over 20 yrs. Thus, initiating a hydraulic fracture along the lateral length of a horizontal well appears to produce greater volumes of gas than three transverse fractures intersecting the lateral length of the horizontal infill wells in the Hugoton field.

### **Compare Fracture Modeling Results – Refined Grids vs. ff factor**

Long run times and convergence problems occur when six infill wells (Figure 11), located such that each section has 4 producing wells, are simulated using six sets of refined grids describing their respective hydraulic fractures. Thus, the ff-factor (in CMG's IMEX simulator) was used to model enhanced well productivity comparable to a hydraulically fractured vertical well. The ff-factor is a multiplier (greater than 1) that applies to the well index and can be varied from layer to layer in IMEX. It allows the user to employ a multiplier on the layer productivity (or injectivity) calculated from input reservoir properties. It also enables increasing the productivity index of the well without creating problems associated with using large negative skins, such as the denominator in the well index equation going negative as skin factor approaches -0.5.

Refined grids describing a hydraulically fractured well do a better job in simulating the initial flush production. The ff-factor does effectively estimate this initial flush production period as it is unable to model accurately the transient linear (and bilinear)

flow (associated with the initial period when fracture volume unloads into the well) which precedes the eventual pseudo steady radial flow.

Figure 12 compares the simulator-calculated production rate from a vertical Flower A1 well with the hydraulic fracture ( $H_f = 325$  ft,  $K_f = 11,000$  md) modeled using refined grids (FlwrVert325 K11000 shown by blue line) with that calculated using ff-factor = 9 (Flwr ff9 shown by red line). As expected, the initial (flush) production rate obtained by the use of the ff-factor is significantly greater than that obtained when refined grids are used to model the fracture. However after the 1<sup>st</sup> year, the rate calculated using ff-factor becomes close and slightly lower than that obtained from the use of refined grids. Over a 20-year period, the calculated cumulative gas produced from Flower A1 using refined grids is 0.689 bcf while that from the use of the ff-factor is 0.679 bcf, a difference of only 1.45% which is well below the margin of error prevalent in the reservoir model in terms of uncertainties regarding facies and permeability distribution in each layer and attendant relative permeability assumptions.

Figure 13 compares results from using refined grids (FlwrVert 162 K11000 shown by the blue line) to model production from a vertical Flower well that is hydraulically fractured (assuming  $H_f = 162$  ft and  $K_f = 11,000$  md) with that calculated by using ff-factor = 5 (Flwr ff5 shown by the red line). As before, the use of the ff-factor results in higher initial (flush) production as compared to that obtained using the refined grids. However as in the previously discussed situation, the difference between rates calculated using the ff-factor and refined grids decrease over time resulting in a difference of 6% in terms of cumulative gas produced over a 20-year period.

Thus, Figures 12 and 13 clearly show that the use of ff-factor to model hydraulic fractures in Hugoton field infill wells results in a quick approximation of average annual production rate (barring the initial flush period) and cumulative production over a 20-year period.

#### **Effects of 4<sup>th</sup> Vertical (Infill) Well per Section**

Figure 12 plots the simulator-calculated production from the Flower A1 (vertical well) using ff = 9 (to approximate effects of a hydraulic fracture with  $H_f = 325$  ft,  $K_f = 11,000$  md [shown by the Flwr&Infills ff9 line in black]) with 6 additional infill (vertical and hydraulically fractured) wells (named with the prefix “Sec” [Figure 11]) positioned such that every section of the Flower area has four producing wells, each starting to produce as of January 1, 2008 in the simulator. Figure 13 similarly plots the production from the Flower A1 (vertical) well using ff-factor = 5 (to approximate effects of a hydraulic fracture with  $H_f = 162$  ft and  $K_f = 11,000$  md [shown by the Flwr&Infills ff5 line in black]) with six additional infill wells in the Flower study area. In each of these cases, the hydraulic fractures at the new infill wells were modeled using the same ff-factor as employed at the Flower well for that run. In both the cases, the use of ff-factor results in overestimation of the initial flush production. However, the calculated production rate during the later years when compared to that from the Flower well without the six additional producing infill wells (shown by the Flwr ff9 curve in red in Figures 12 and

13) clearly shows that interference occurs at the Flower well when each section is produced by four wells, i.e., an additional infill well.

Figure 14 shows maps of simulator-calculated pressure distribution in the Fort Riley layer, one of the layers from which significant volumes of gas (about 25%, Figure 6) is estimated to flow out in the post-2008 period. Comparison of Figure 14B and 14C show that infill wells (such as the 4<sup>th</sup> well per section which start to produce in the simulator as of Jan 1, 2008) cause significant incremental gas production resulting in decline in reservoir pressure in the Fort Riley layer by January 1, 2018. Figure 14D plots the simulator-calculated pressure in the same layer as of January 1, 2028, after drainage by existing and additional infill wells, and when compared with Figure 14C, indicates that the above infill wells continue to produce additional incremental gas from the Fort Riley beyond January 1, 2018.

The average annual production rate and the cumulative production from the infill wells (including Flower A1) all completed as hydraulically fractured vertical wells are shown in Figures 15A and B. Figure 15A displays the average annual production rate from these wells modeled using ff-factor = 9 (i.e., approximating the effects of a fracture with  $H_f = 325$  ft and  $K_f = 11,000$  md), while Figure 15B displays the average annual production rate from these wells modeled using ff-factor = 5 (i.e., approximating the effects of a fracture with  $H_f = 162$  ft and  $K_f = 11,000$  md). These simulation results indicate that a hydraulically fractured infill vertical well in the Flower area will recover about 0.5 bcf of gas over 20-year period.

### **Incremental Gas Recovery by Infill Drilling**

Figure 16 compares the simulator-calculated average annual production rate from 2008 to 2028 at the Chase Parent wells (whose names carry the prefix “P”) with and without the production from seven infill wells (including Flower A1) located such that each section in the Flower area has four wells. The simulator-calculated average annual production rate at the Chase Parent well without the infill wells is shown in red while the resulting production from seven infill wells is shown in dark blue (where hydraulic fracture at infill wells are modeled using ff-factor = 5 to approximate  $H_f = 162$  ft and  $K_f = 11,000$  md) and light blue (where hydraulic fracture at the infill wells are modeled by using ff-factor = 9 to approximate  $H_f = 325$  ft and  $K_f = 11,000$  md). The intent of this comparison is to show the presence or absence of interference effects at the existing Chase Parent wells as a result of having four wells produce per section in the Flower area from January 1, 2008. The plots show that the presence of a 4<sup>th</sup> infill well (per section) results in interference, and thus decreases the anticipated production from the existing Chase wells. The decrease in production (from what is expected from these wells if the infills [additional 4<sup>th</sup> well per section] were not drilled) is around a few mcf/d in the initial years (after 2008), and reaches a maximum of around 10 mcf/d in the later years for some of the Chase Parent wells. Figure 17 similarly plots the interference effects at the existing Council Grove wells as a result of the drilling of seven vertical infill wells located such that each section in the study area has four producing wells. Like the Chase Parent wells, varying degrees of interference is also noted at the existing Council Grove wells. The

interference is minimal (i.e., decline of a few mcf/d or less) during the initial years (after 2008) and reaches a maximum of around 20 mcf/d in some of the wells in the later years.

Tables in Figure 18 compare the incremental gas produced from seven infill (vertical) wells, drilled such that each section in the Flower area has four producing wells, with lost production volumes at the existing Chase and Council Grove wells as a result of interference over a 20-year period (2008 to 2028). Figure 18A shows that cumulative production from existing Chase Parent wells (names prefixed with “P”) without the infill wells is around 3.129 bcf while that as a result of interference from seven infill wells was 2.711 bcf (using ff-factor = 9 at the infill wells to approximate hydraulic fractures with  $H_f = 325$  ft and  $K_f = 11,000$  md) and 2.762 bcf (using ff-factor = 5 at the infill wells to approximate hydraulic fractures with  $H_f = 162$  ft and  $K_f = 11,000$  md), respectively. Thus if the infill wells are modeled using ff-factor = 5 and 9, the lost production from existing Chase Parent wells is 0.367 and 0.418 bcf, respectively. Similarly, Figure 18B shows that the volume of lost (gas) production from existing Council Grove wells is 0.594 and 0.67 bcf when the hydraulic fractures at the seven infill wells is modeled using ff-factor = 5 and 9, respectively. Figure 18C summarizes the cumulative production from each of the 7 infill wells, and shows that the total recovery from these wells over the 20-year period is 4.637 and 4.083 bcf, respectively, depending on the assumptions made about the hydraulic fractures at these wells, i.e.,  $H_f = 325$  ft or 162 ft and  $K_f = 11,000$  md. Figure 18D balances the production gained from these infill wells against that lost from existing Chase and Council Grove wells due to interference, and it shows an incremental recovery of 3.549 and 3.122 bcf, respectively, depending on assumptions made about the effectiveness of the hydraulic fractures (i.e.  $H_f = 325$  ft or 162 ft and  $K_f = 11,000$  md) at the infill wells. This mass balance over nine sections around the Flower A1 well translates to a recovery of 0.35 to 0.39 bcf per section over a 20-year period based on the ff-factor used (i.e., 5 or 9) to model hydraulic fractures at the infill wells.

### **P/z Plot – Incremental Recovery & Interference**

Figure 19 plots the simulator-calculated average P/z over the hydrocarbon pore volume (in all layers) in the nine-section area around the Flower A1 well since the onset of production in 1938 until 2028. The simulator geomodel history-matched available production data from Chase Parent and Council Grove wells in the study area between 1938 and July 2003. Thereafter the wells were flowed under pressure constraints. Also, the model matched available layer pressure data and well-level flowing pressures.

The last of the Chase Parent wells was completed in October 1953, and thereafter the average P/z for the Flower area went into a linear decline till the onset of the drilling of Council Grove wells (in May 1970) which resulted in a change in slope (with a steeper decline) of the P/z curve. The onset of drilling of the Chase Infill wells in January 1988 resulted in a change in the P/z slope again with a steeper decline. Thus each round of new drilling activity in the Hugoton field appears to cause a change in the P/z slope marked by a steeper decline indicating incremental recovery of gas. If all the additional gas produced by a new set of wells was equal to the reduction in produced volumes from existing wells, the P/z slope would remain unchanged. Thus downward inflections of the P/z

curve, particularly when the new slope is steeper than that previously established, indicate that previously unmobilized incremental gas is being produced by the new series of wells despite presence of interference.

The final series of (hypothetical) wells drilled in this area consisted of the seven infill vertical wells (including Flower A1) that were completed in the simulator as of January 1, 2008. These wells were placed such that the each section in the Flower area would have four producing wells, and were produced in the simulator till 2028. Figure 19 and 20 compares the hydrocarbon pore volume weighted average of the Flower area P/z with no infill drilling (shown by the curve in red) with that obtained when seven infill wells were drilled as of January 1, 2008, in the simulator and whose fractures were modeled using ff-factor = 5 (shown in green and approximates  $H_f = 162$  ft and  $K_f = 11,000$  md) and ff-factor = 9 (shown in blue and approximates  $H_f = 325$  ft and  $K_f = 11,000$  md). The narrower time scale (X- axis) in Figure 20 shows that infill drilling inflects the P/z curve downward and results in steepening of the P/z decline. However, Figure 19 shows that as compared to previous rounds of drilling, the change in the P/z decline slope is the least for this round of 4<sup>th</sup>-well-per-section series of wells. This may indicate that as compared to previous rounds of drilling activity, the new round of 4<sup>th</sup>-well-per-section drilling will be least effective in producing unmobilized (new) gas. This is expected because the Hugoton field is quite mature and majority of the residual reserves remain in low-permeability zones with poorer recovery efficiencies.

## Conclusions

1. The most critical factor affecting recovery from hydraulically fractured infill wells in the Flower area is the producing fluid column because flow rates (and therefore cumulative production) are significantly affected by the back pressure exerted by as small as 30 ft of fluid column in the well.
2. The hydraulic fracturing should be designed to attain maximum half-length ( $H_f$ ) and high fracture permeability ( $K_f \geq 8000$  md).
3. In the post-2008 period, gas production from existing and infill wells is dominated by contributions made from tighter layers such as Towanda, Fort Riley, Wreford, and Lower Fort Riley. Volume of gas moving out of these layers is around 75% of the total gas flow in the reservoir.
4. Under the conditions simulated, the simulator-calculated cumulative production over 20 years from a horizontal Flower A1 well laterally fractured exceeds that from the same well completed vertically and hydraulically fractured by no greater than 1.7 times.
5. The simulator-calculated production from a horizontal Flower A1 well hydraulically fractured along its lateral length exceeds that when the same well is intersected by three transverse fractures (with similar characteristics) placed at the toe, mid-section, and the heel.
6. Barring the initial flush production period, the ff-factor quickly estimates the approximate rate and cumulative production (over 20 years) of a hydraulically fractured vertical infill well in the Flower area.

7. Production from the Flower well is affected (by interference) due to the drilling of an additional 4<sup>th</sup>-well-per-section in the Flower area.
8. A hydraulically fractured infill vertical well in the Flower area is expected to recover about 0.5 bcf of gas over 20-year period based on simulator-calculated results.
9. A mass balance of gas produced from infill wells and volumes lost from existing wells (Chase Parent and Council Grove) due to interference from the infill wells shows that at least 0.35 bcf of incremental gas is expected to be produced per section (over 20 years based on simulation results) as a result of drilling an additional well in each section in the Flower study area.
10. That additional (otherwise unmobilized) gas is produced as a result of drilling the 4<sup>th</sup>-well-per-section despite creating interference at existing wells is also confirmed by the plot of P/z (averaged over all layers in the study-area using grid hydrocarbon [HC] pore volume) over time, which shows a downward inflection and steepening of the slope after onset of production from the above mentioned infill wells.

**Reference:**

Bhattacharya, S., Dubois, M., and Byrnes, A., 2005: Reservoir characterization of 9-Section area around Flower A1 well – Chase/Council Grove Reservoir Systems, KGS OFR 2005-54

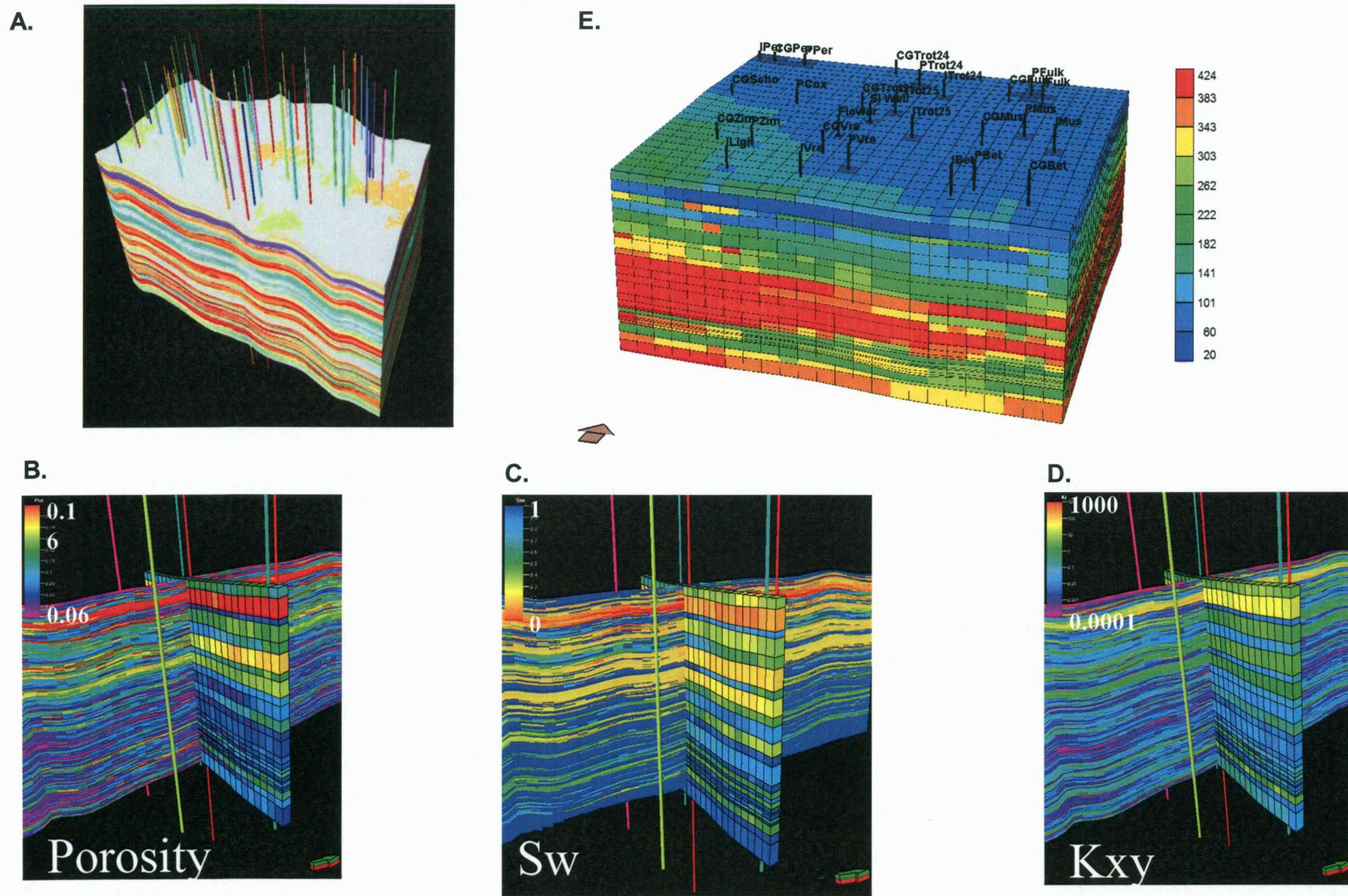


Figure 1. A) View of the coarse scale model built over a large area around the Flower A1 well. B) Cross-section showing upscaling of porosity. C) Cross-section showing upscaling of water saturation ( $S_w$ ). D) Cross-section showing upscaling of permeability ( $K_{xy}$ ). E) 25-layer coarse model that served as the base for reservoir simulation studies.

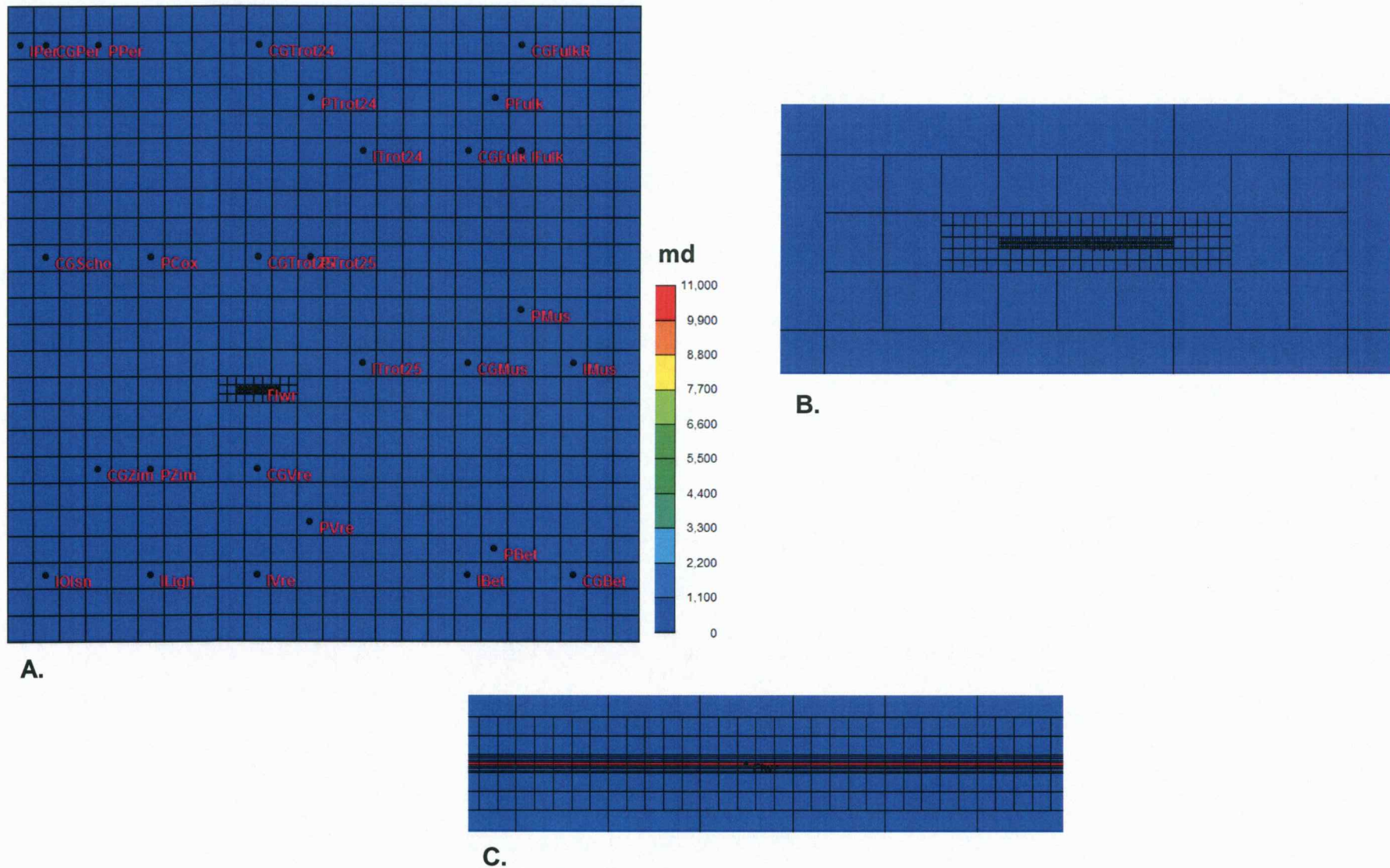


Figure 2. A) Map showing location of the Flower A1 (Flwr) well in the Flower simulation area. B) Distribution of refined grids around the Flwr well to define the hydraulic fracture. C) The modeled hydraulic fracture is defined using 1ft by 8.8 ft (refined) grid cells that are colored in red (showing a fracture permeability of 11,000 md in red).

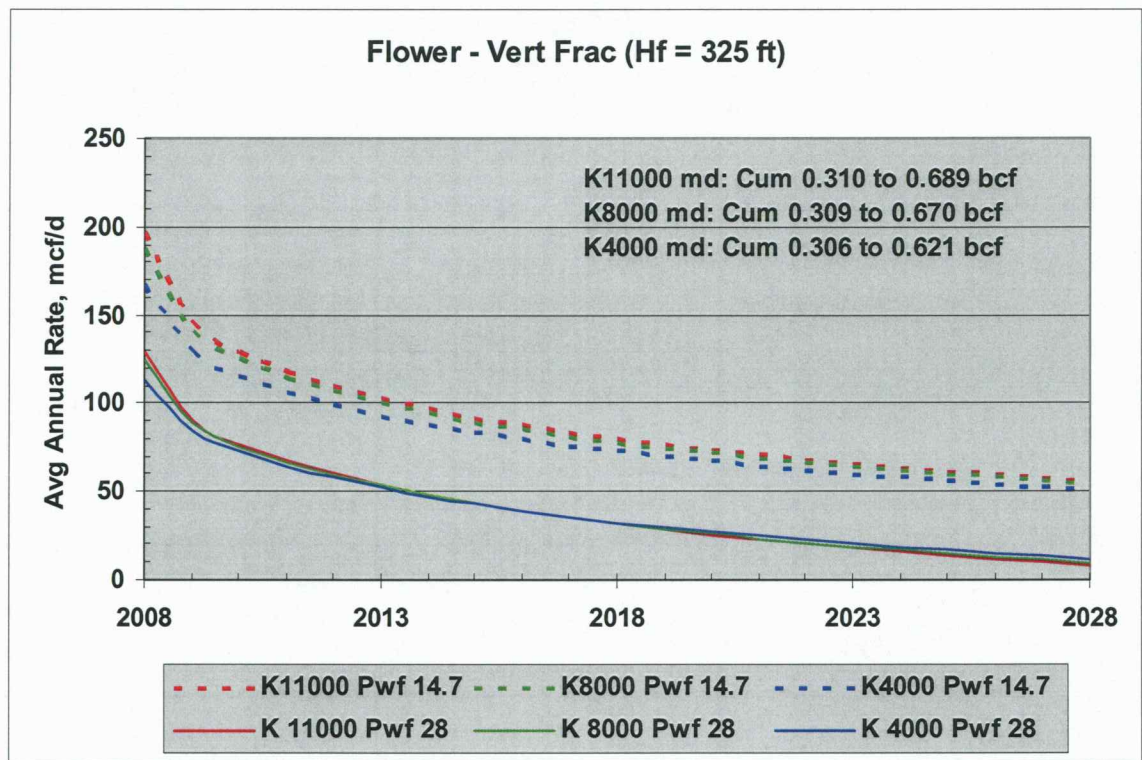
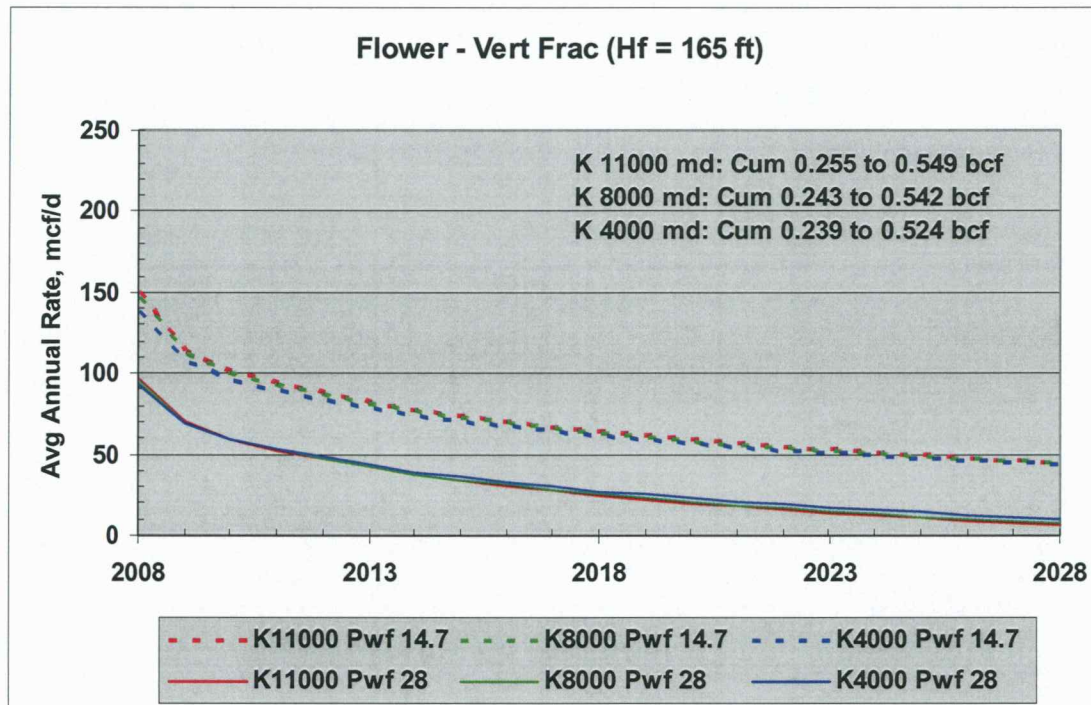


Figure 3. Plot showing average yearly production (rate) from Flower A1 well with a hydraulic fracture half-length of 325 ft and fracture permeability varying from 4000 md to 11,000 md. Broken lines refer to producing the Flower A1 well at bottom-hole pressure (BHP) of 14.7 psi while the unbroken lines refer to BHP = 28 psi.



**Figure 4. Plot showing average yearly production (rate) from Flower A1 well with a hydraulic fracture half-length of 165 ft and fracture permeability varying from 4000 md to 11,000 md. Broken lines refer to producing the Flower A1 well at bottom-hole pressure (BHP) of 14.7 psi while the unbroken lines refer to BHP = 28 psi.**

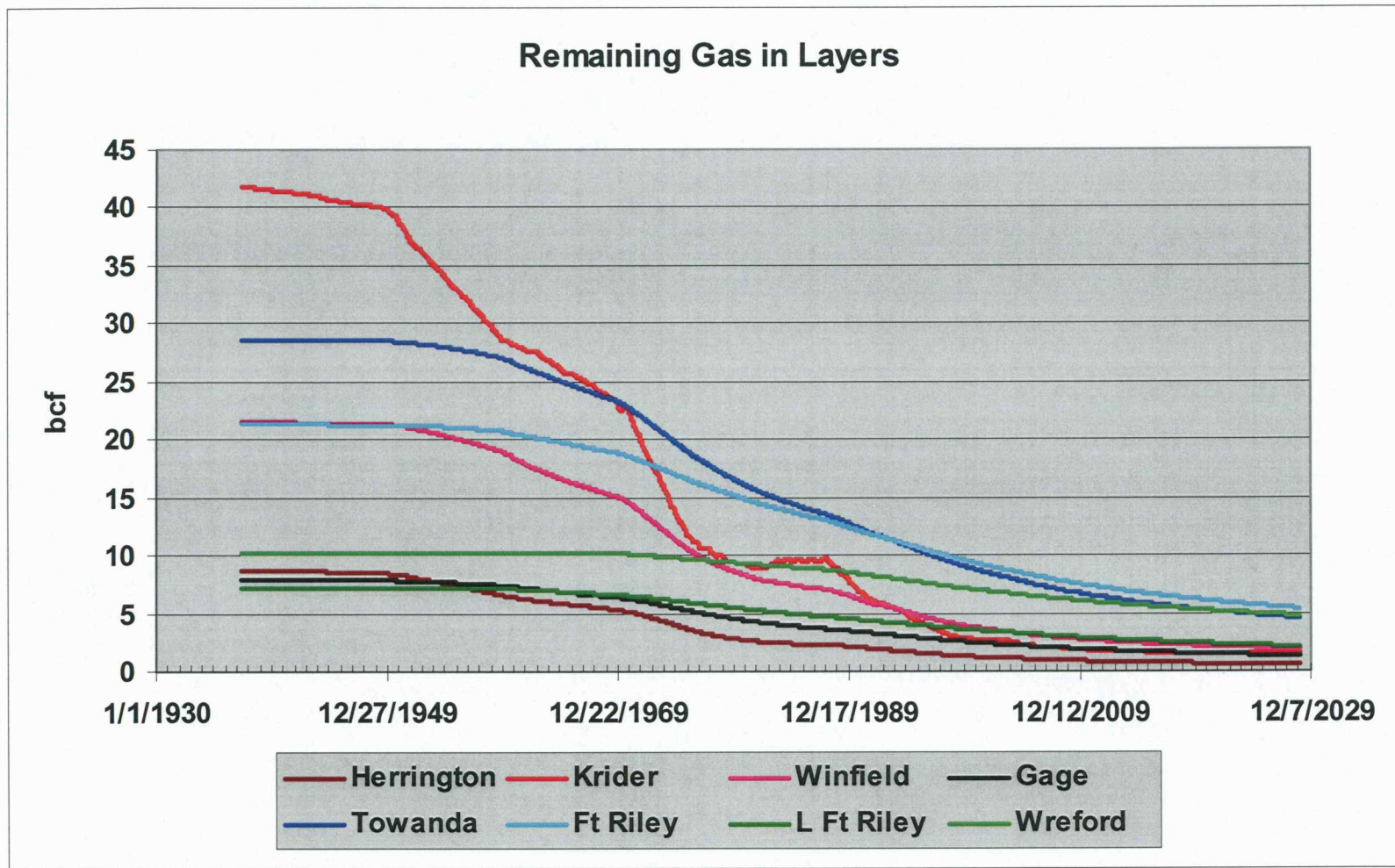


Figure 5. Plot showing the simulator-calculated remaining gas in each of the respective layers in the 9-section area around the Flower A1 well. In this model, the Flower A1 well begins to produce (at bottom hole pressure of 14.7 psi) as of January 1, 2008 with a fracture permeability of 11,000 md and half-length of 325 ft.

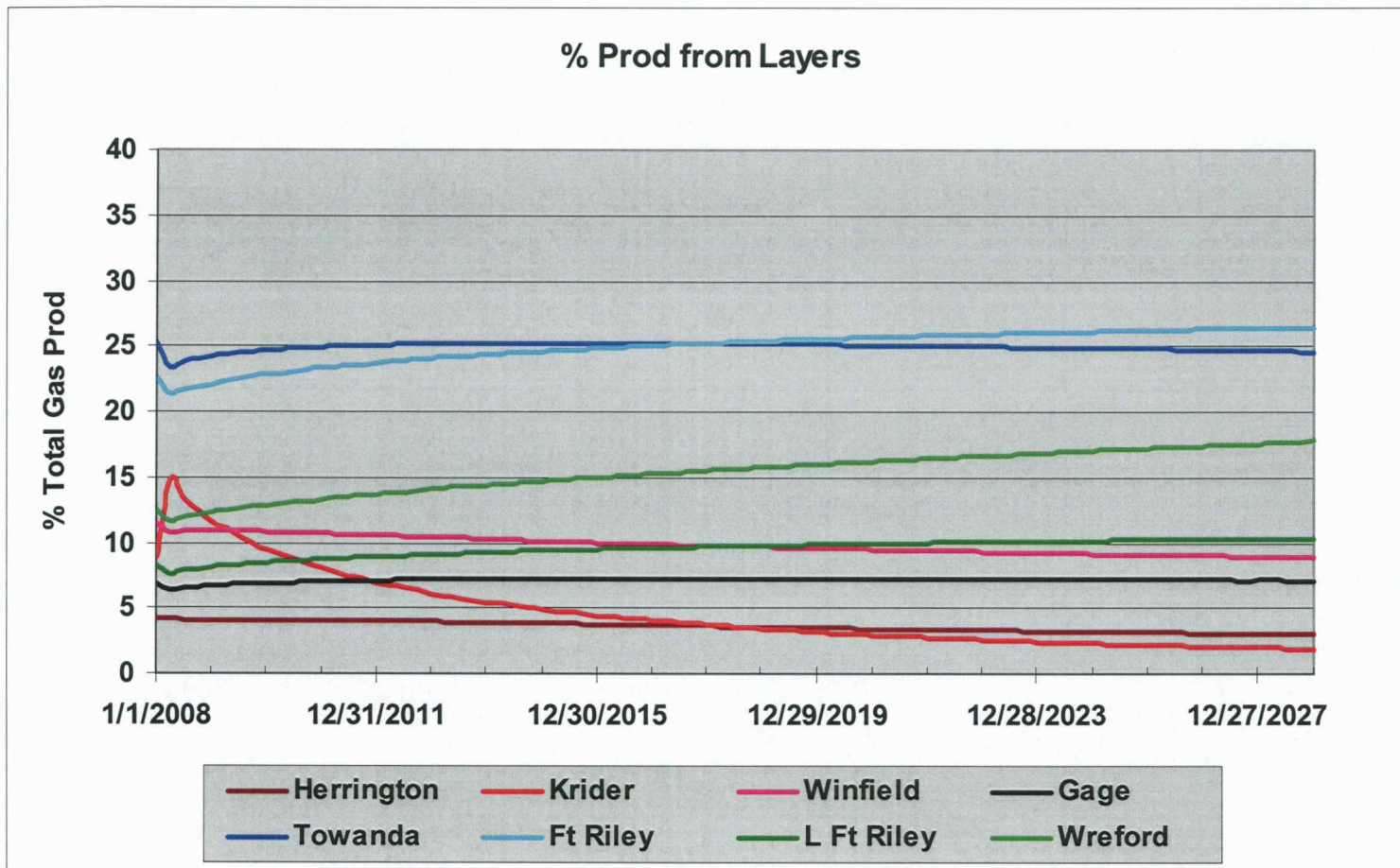


Figure 6. Plot showing the percentage contribution of each layer to the total volume of gas moving out of all the stated layers in the post-2008 period. The data plotted here has been obtained from the simulation results plotted in Figure 4.

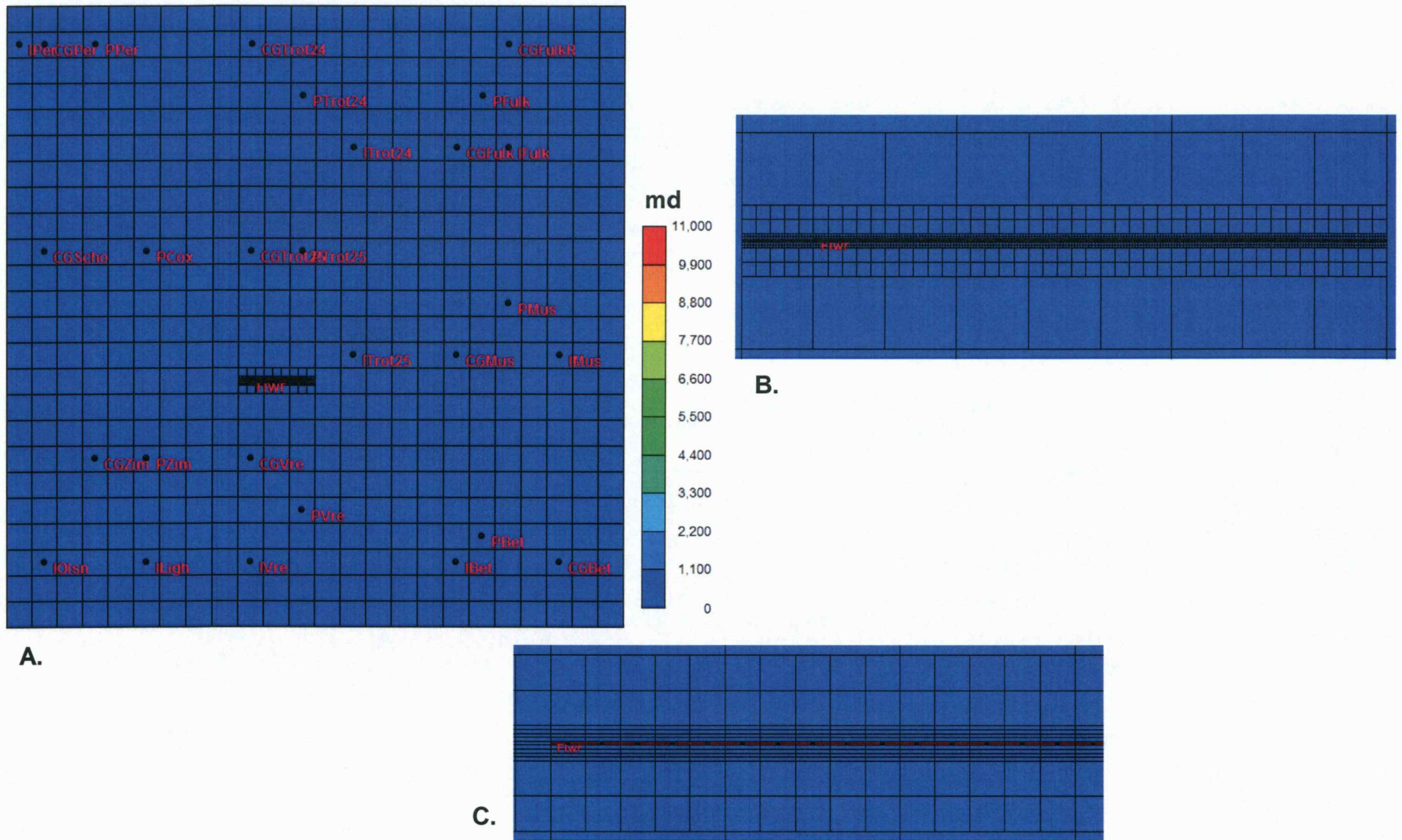


Figure 7. A) Map showing location of the Flower A1 (Flwr) horizontal well in the Flower simulation area. B) Distribution of refined grids around the Flwr well to define the hydraulic fracture along the lateral length of the well of 1500 ft. C) The modeled hydraulic fracture is defined using 1ft by 8.8 ft (refined) grid cells that are colored in red (showing a fracture permeability of 11,000 md in red).

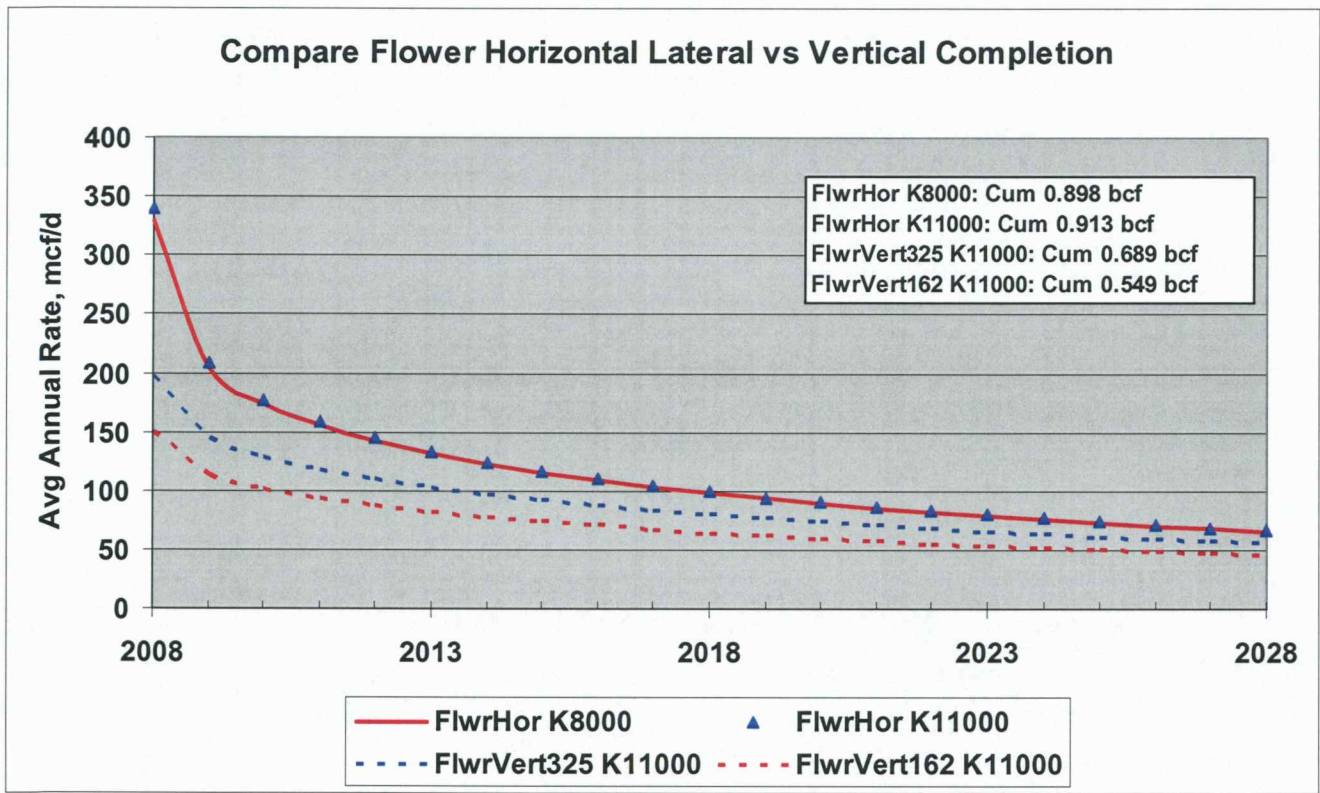
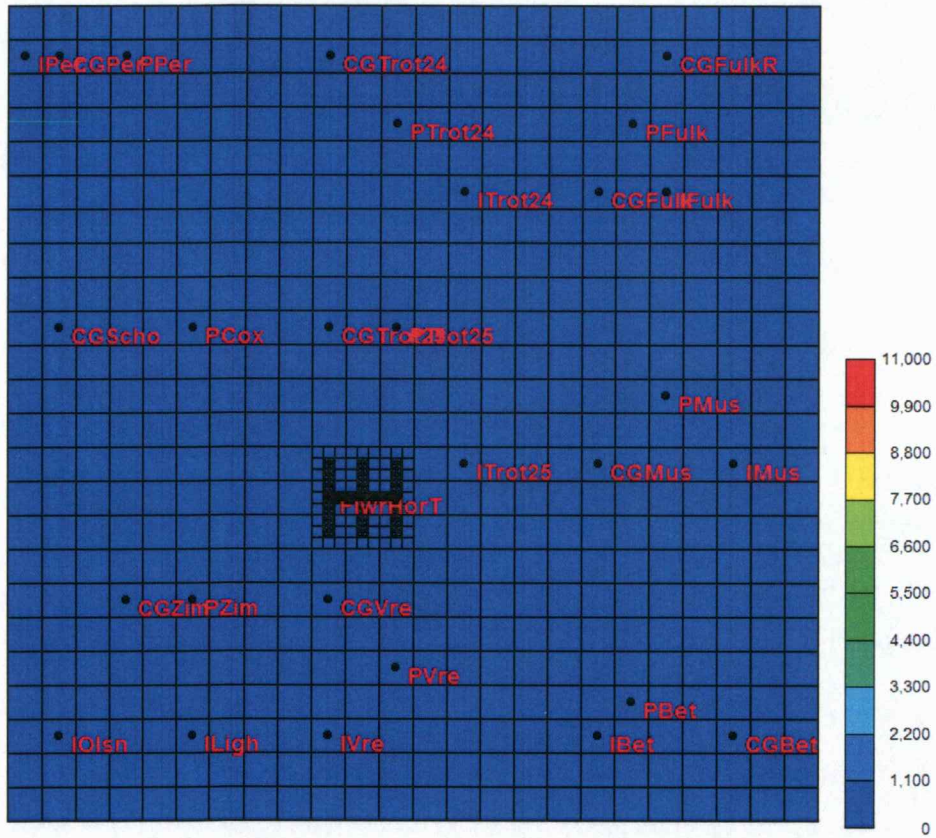
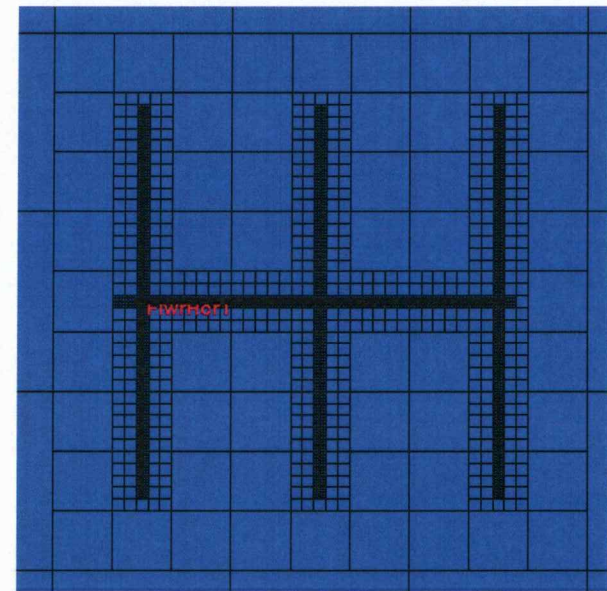


Figure 8. Plot comparing the simulator-calculated average annual production rate from Flower horizontal well 1500 ft long and completed as a laterally fractured well along its length. Production rates were calculated assuming two sets of fracture permeability ( $K_f$ ), i.e.,  $K_f = 11,000$  md (blue triangles) and  $K_f = 8000$  md (red line).



B.



C.

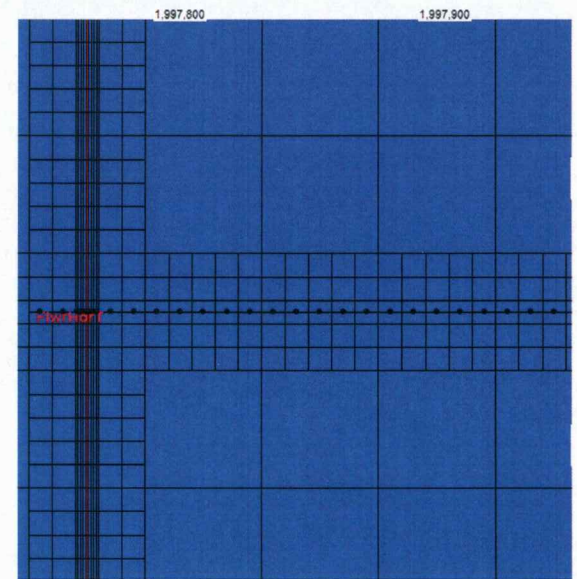


Figure 9. A) Map showing location of the Flower A1 (Flwr) horizontal well in the Flower simulation area. B) Distribution of refined grids around the Flwr well to define the transverse hydraulic fractures intersecting horizontal well of 1500 ft. C) The modeled hydraulic fracture is defined using 1ft by 8.8 ft (refined) grid cells that are colored in red (showing a fracture permeability of 11,000 md in red).

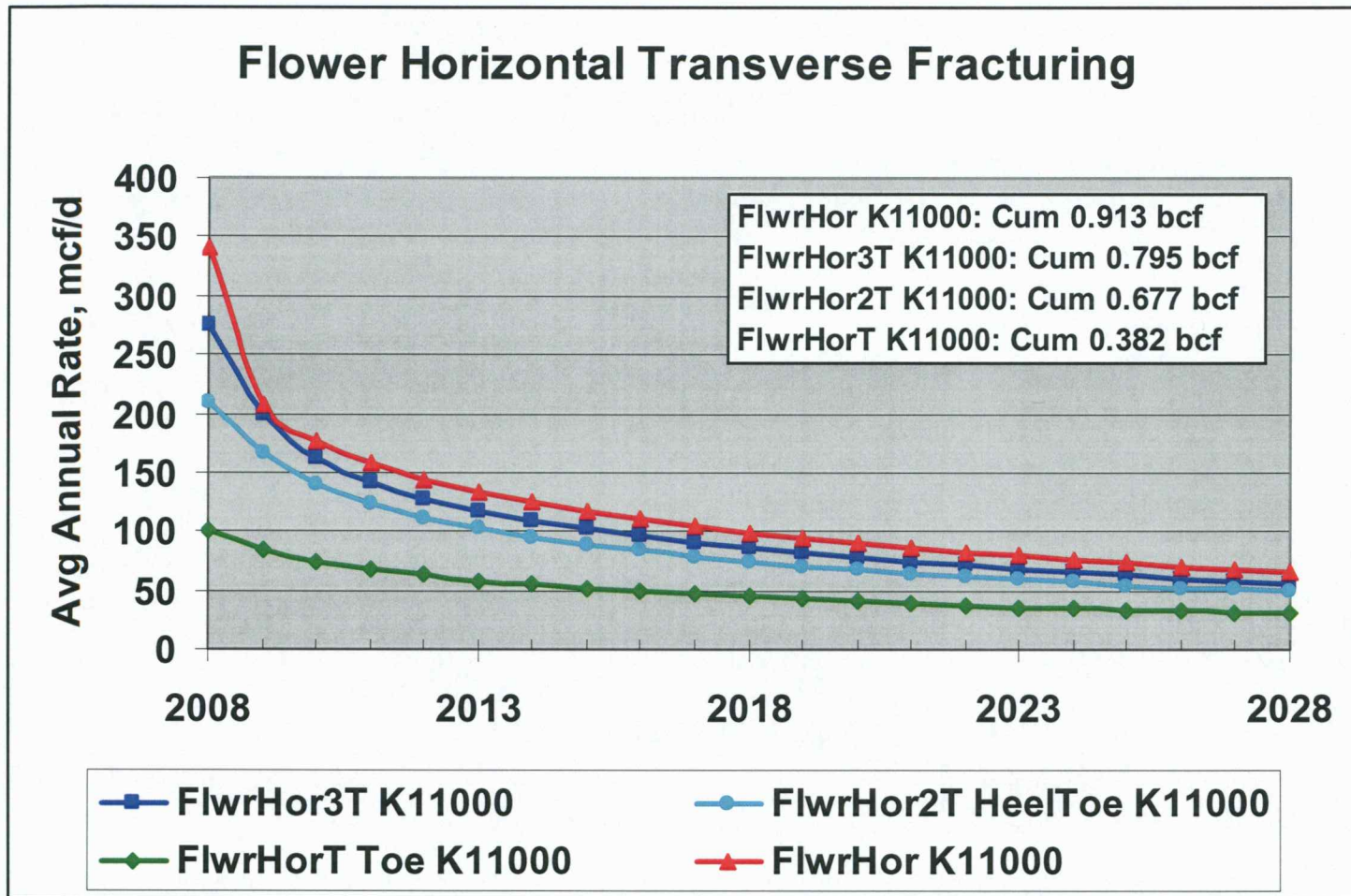


Figure 10. Plot comparing the simulation-calculated average annual production rate for Flower horizontal well having one transverse fracture at the toe (FlwrHorT), two transverse fractures at heel and toe (FlwrHor2T), and three transverse fractures at heel, mid-section, and toe (FlwrHor3T) with a Flower horizontal well that was fractured along its lateral length (FlwrHor) of 1500 ft. For transverse fractures, the fracture half-length was 750 ft and the fracture permeability was assumed to be 11,000 md for all runs.

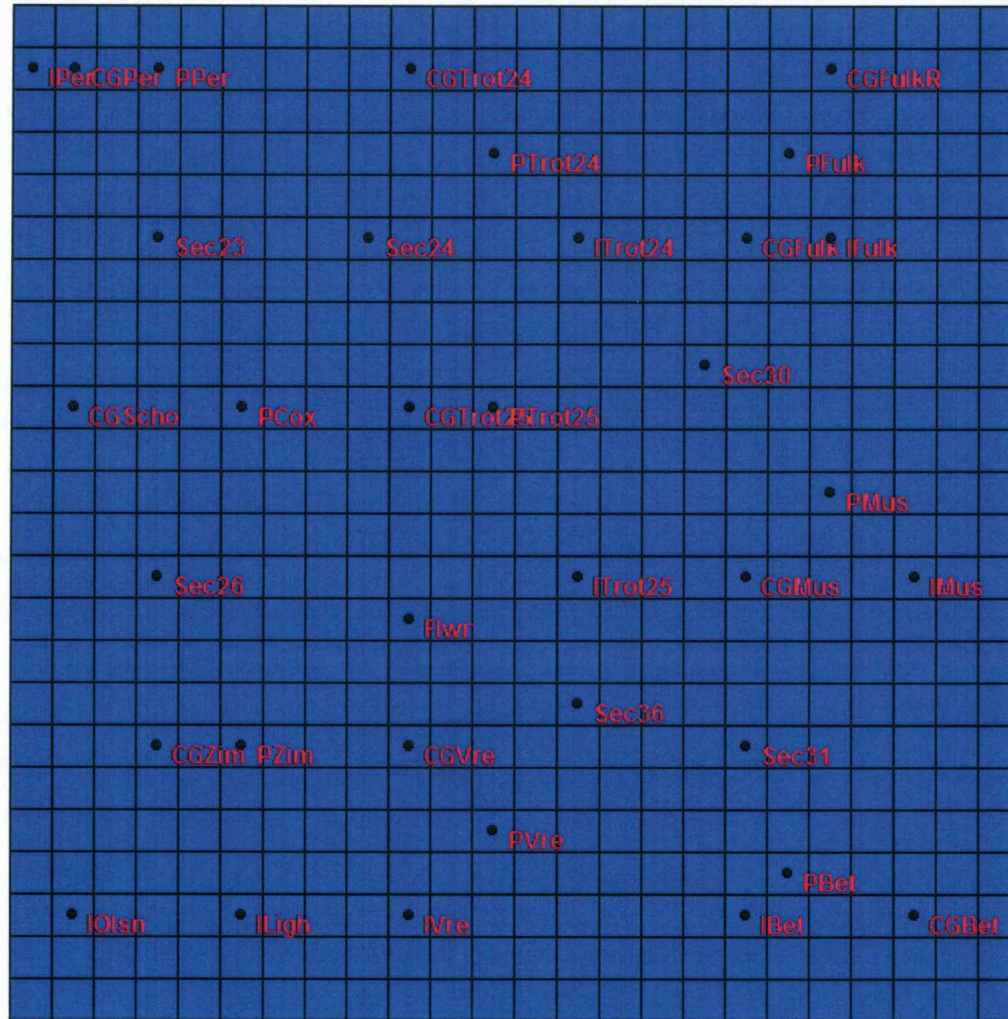


Figure 11. Map showing the location of the existing wells - Chase (names with prefixes “P” and “I”) and Council Grove (names with prefix “CG”). Also, shown are location of seven infill wells (named as Flwr, Sec 23, Sec 24, Sec 26, Sec 30, Sec 31, and Sec 36) placed such that each section has four producing wells.

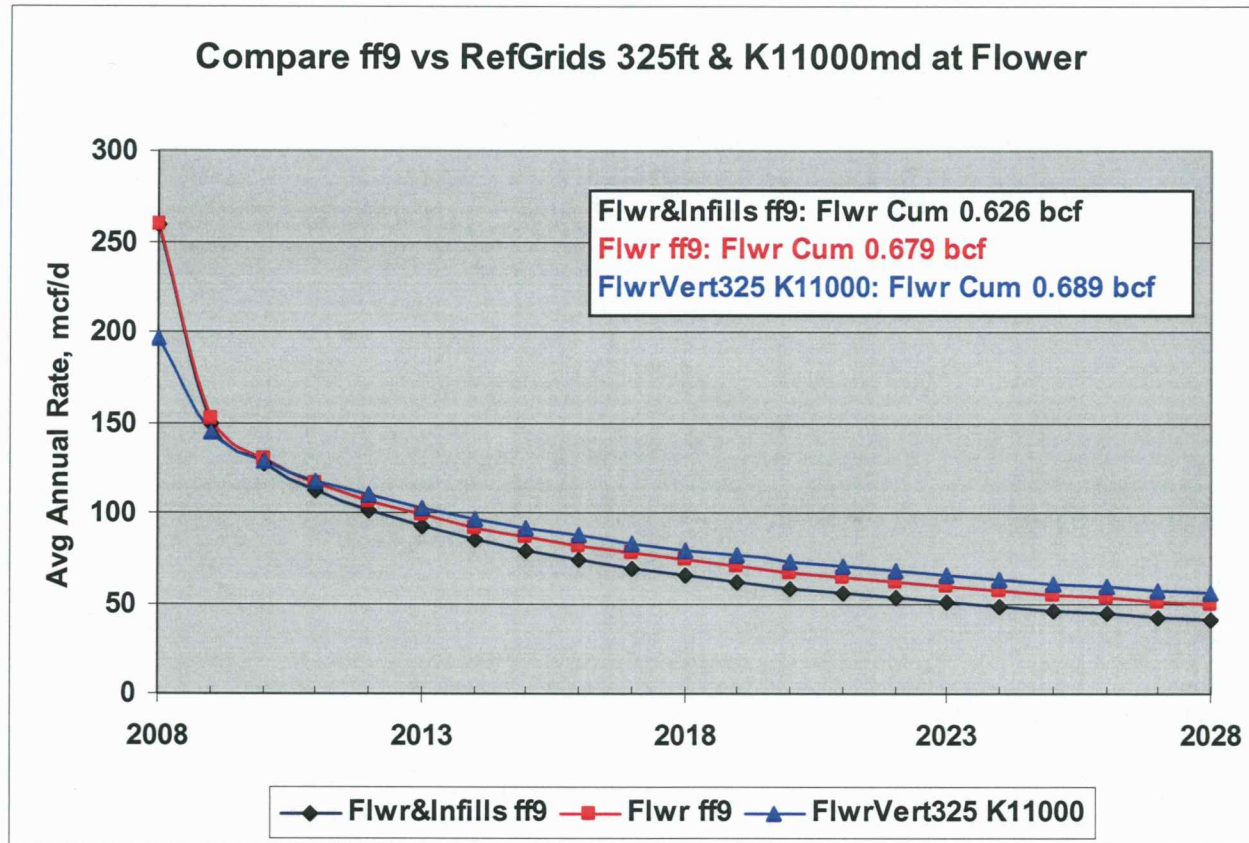


Figure 12. Plot of simulated production from a hydraulically fractured vertical Flower A1 well. The plot compares calculated production rate from the well obtained by using refined grids (FlwrVert325 K11000 in blue) to delineate the fracture (half-length of 325 ft and permeability of 11,000 md) against that by using ff-factor = 9 (Flwr ff9) in red. Also plotted for comparison and show of interference is the calculated production rate from Flower (Flwr&Infills ff9 in black) when six other infill wells (each modeled with ff = 9) are placed on production (as of January 1, 2008) such that each section has four wells.

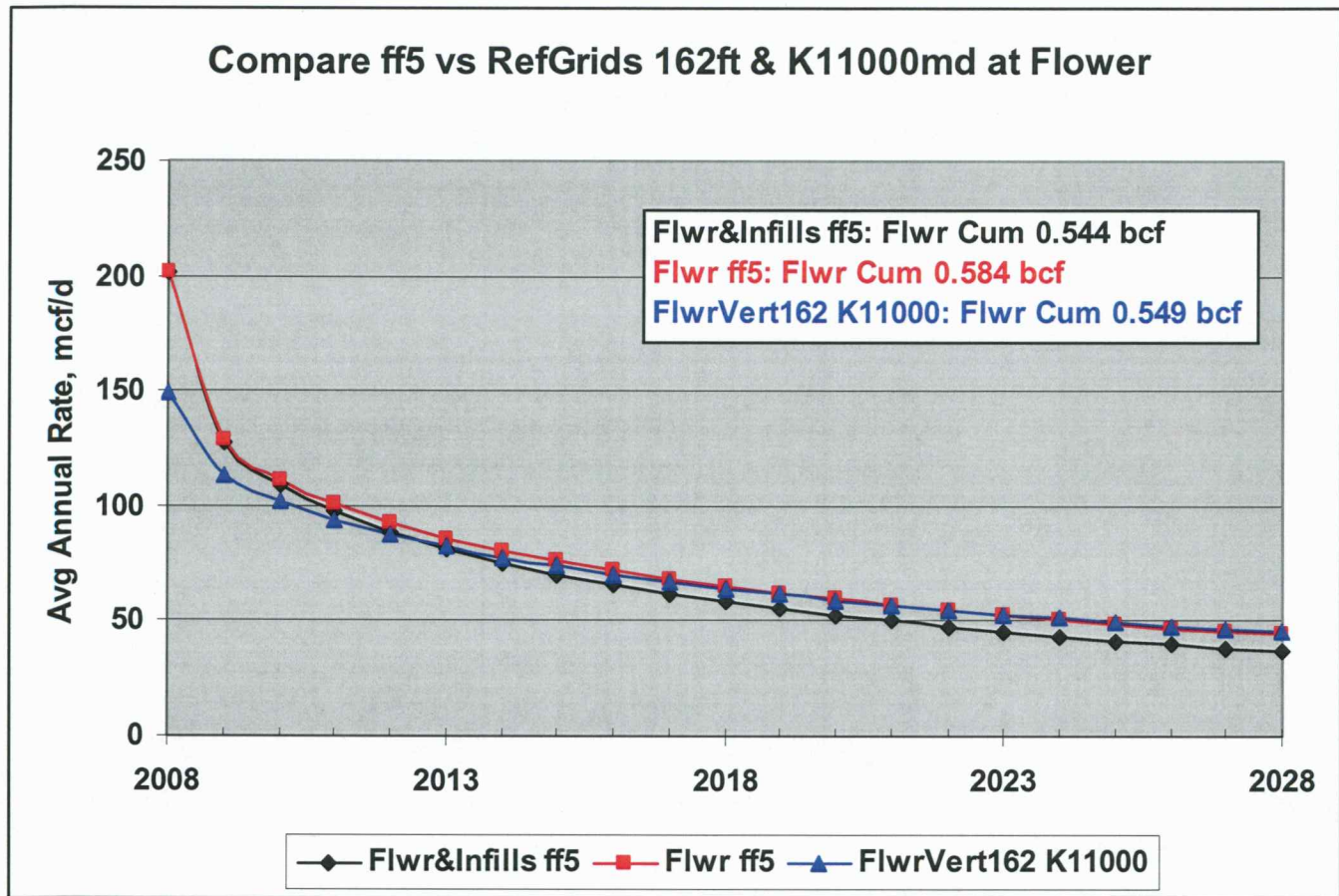
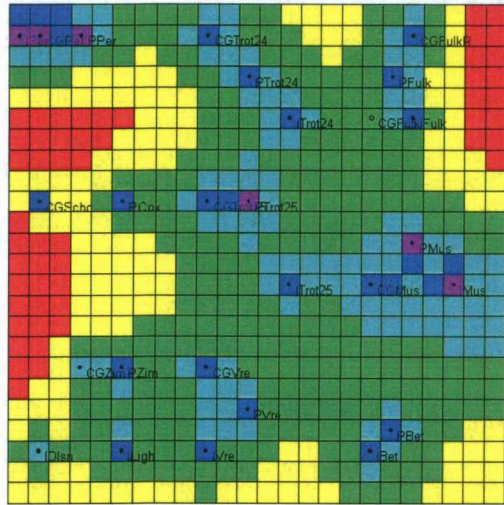
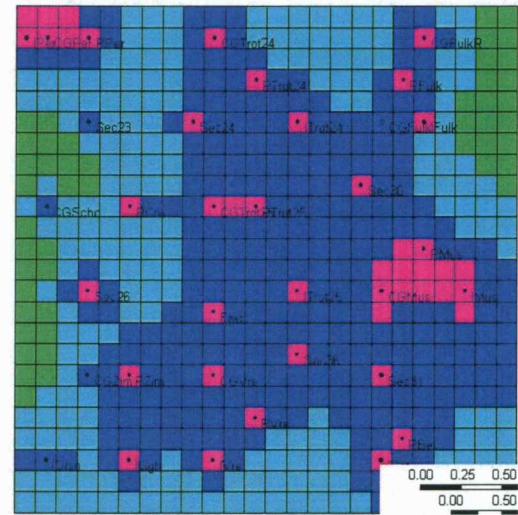


Figure 13. Plot of simulated production from a hydraulically fractured vertical Flower A1 well. The plot compares calculated production rate from the well obtained by using refined grids (FlwrVert162 K11000 in blue) to delineate the fracture (half-length of 162 ft and permeability of 11,000 md) against that by using ff-factor = 5 (Flwr ff5) in red. Also plotted for comparison and show of interference is the calculated production rate from Flower (Flwr&Infills ff5 in black) when six other infill wells (each modeled with ff = 5) are placed on production (as of January 1, 2008) such that each section has four wells.

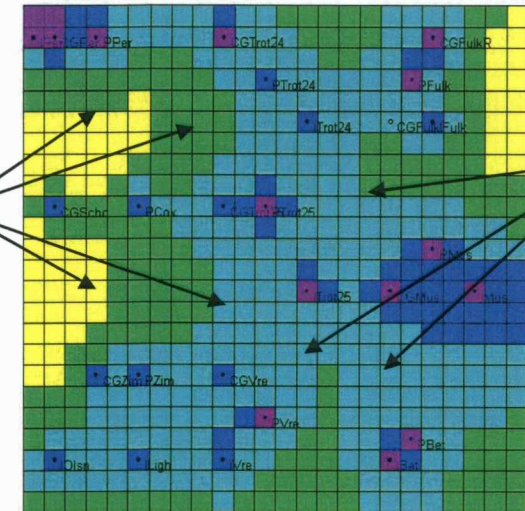
**A. Pressure in Ft. Riley – Jan 1 2008 (No Infills)**



**D. Pressure in Ft. Riley – Jan 1 2028 (Infills, ff9)**

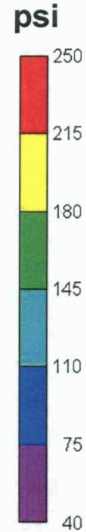


**B. Pressure in Ft. Riley – Jan 1 2018 (No Infills)**



Infill Locations

Infill Locations



**C. Pressure in Ft. Riley – Jan 1 2018 (Infills, ff9)**

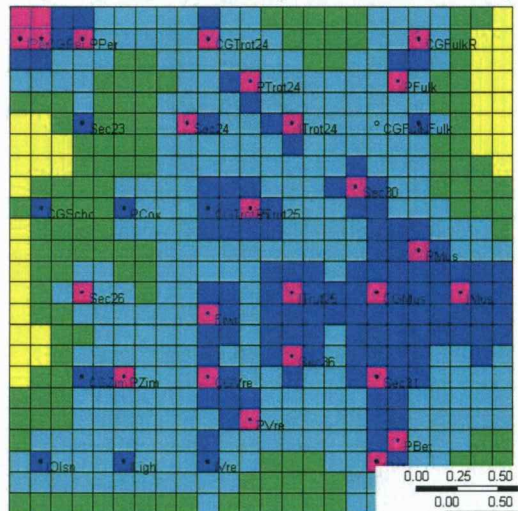
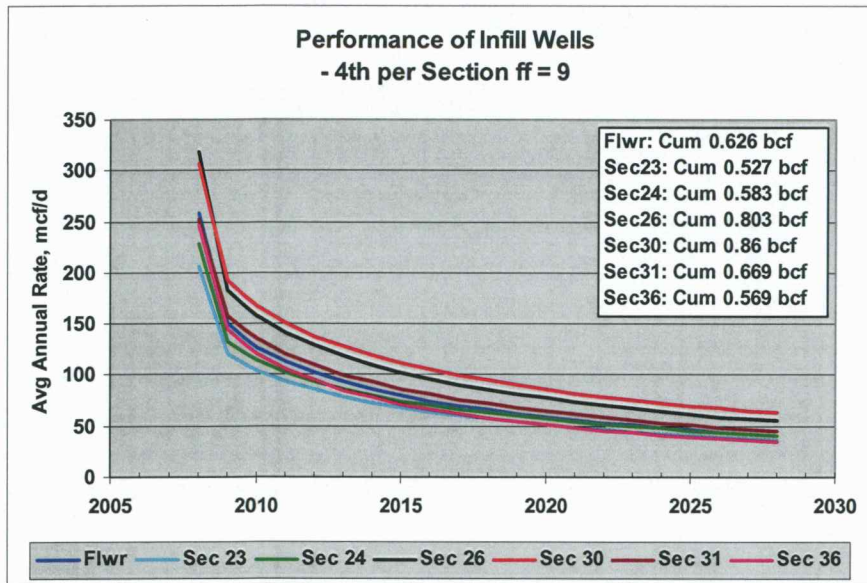
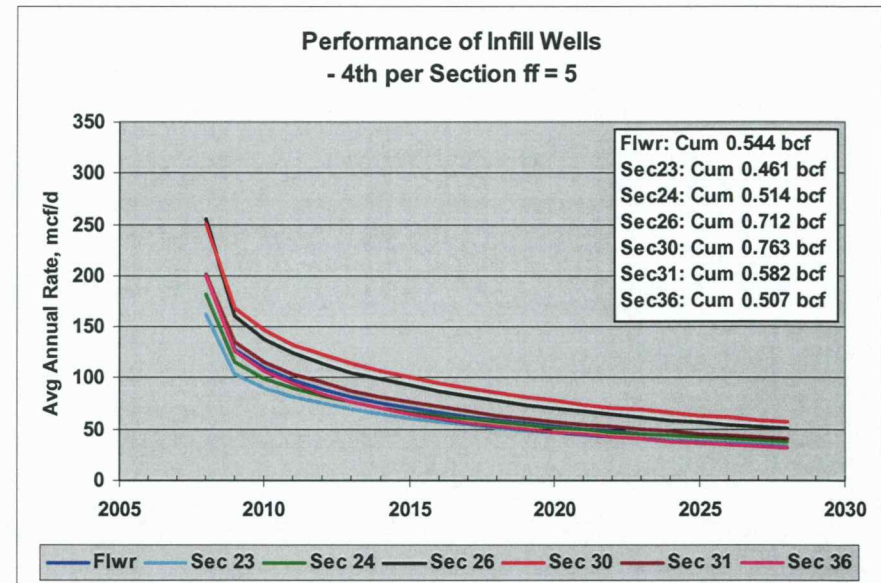


**Figure 14 . A) Map showing the simulator-calculated pressure distribution in Fort Riley layer in the Flower study area as of January 1, 2008. B) Map showing future (simulator-calculated) pressure distribution in Fort Riley as of January 1, 2018, as a result of production from existing Chase and Council Grove wells (and no additional infill wells). C) Future (simulator-calculated) pressure distribution in Fort Riley as of January 1, 2018, as a result of production from existing wells and additional infill wells (an additional 4<sup>th</sup> well per section plus Flower A1 modeled with ff = 9) . D) Future (simulator-calculated) pressure distribution in Fort Riley as of January 1, 2028, as a result of production from existing wells and additional infill wells (an additional 4<sup>th</sup> well per section plus Flower A1 modeled with ff = 9).**



A.



B.

Figure 15. A) Plot showing the average annual gas production rate from the infill wells (placed such that each section in the Flower area has 4 producing wells) that have been completed vertically and fractured and modeled using ff-factor = 9 (to approximate  $H_f = 325$  ft and  $K_f = 11,000$  md). B) Plot showing the average annual gas production rate from the infill wells (placed such that each section in the Flower area has 4 producing wells) that have been completed vertically and fractured and modeled using ff-factor = 5 (to approximate  $H_f = 162$  ft and  $K_f = 11,000$  md).

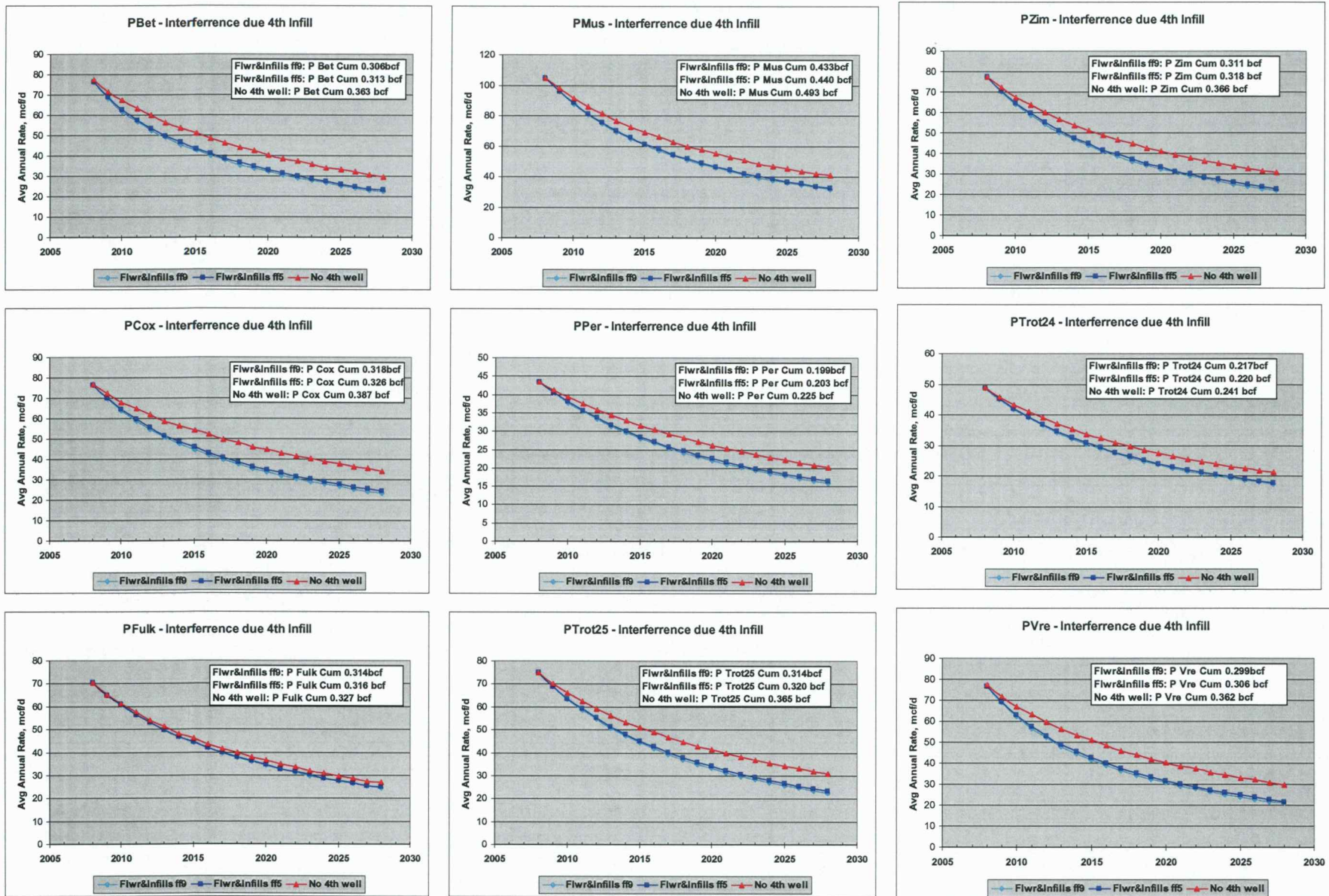


Figure 16. Plots comparing the average annual production rate at existing Chase Parent wells in the Flower area without (shown in red line) and with (shown in dark blue [ff-factor = 5] and light blue [ff-factor = 9]) the drilling of six infill vertical wells (including Flower A1) located such that each section in the study area has four producing wells. Hydraulic fractures at the infill wells were modeled using the ff-factor.

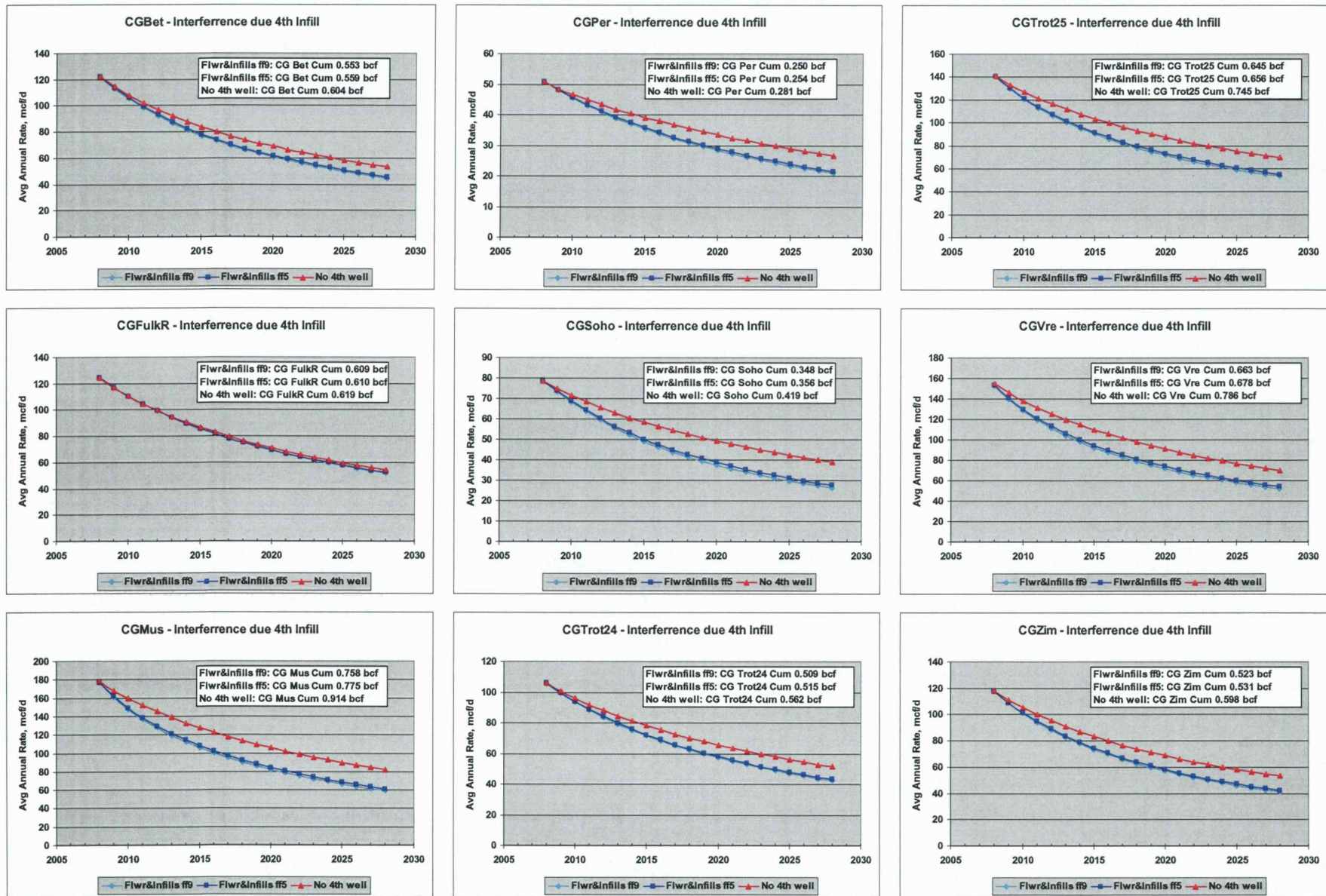


Figure 17. Plots comparing the average annual production rate at existing Council Grove wells in the Flower area without (shown in red line) and with (shown in dark blue [ff-factor = 5] and light blue [ff-factor = 9]) the drilling of six infill vertical wells (including Flower A1) located such that each section in the study area has four producing wells. Hydraulic fractures at the infill wells were modeled using the ff-factor.

|                        | 4th well - ff9 | 4th well - ff5 | No 4th Well  |
|------------------------|----------------|----------------|--------------|
| P Bet, bcf             | 0.306          | 0.313          | 0.363        |
| P Cox, bcf             | 0.318          | 0.326          | 0.387        |
| P Fulk, bcf            | 0.314          | 0.316          | 0.327        |
| P Mus, bcf             | 0.433          | 0.44           | 0.493        |
| P Per, bcf             | 0.199          | 0.203          | 0.225        |
| P Trot25, bcf          | 0.314          | 0.32           | 0.365        |
| P Zim, bcf             | 0.311          | 0.318          | 0.366        |
| P Trot24, bcf          | 0.217          | 0.22           | 0.241        |
| P Vre, bcf             | 0.299          | 0.306          | 0.362        |
| <b>Total CH P, bcf</b> | <b>2.711</b>   | <b>2.762</b>   | <b>3.129</b> |
| <b>Loss CH P, bcf</b>  | <b>0.418</b>   | <b>0.367</b>   |              |

A.

|                      | 4th well - ff9 | 4th well - ff5 | No 4th Well  |
|----------------------|----------------|----------------|--------------|
| CG Bet, bcf          | 0.553          | 0.559          | 0.604        |
| CG Fulk R, bcf       | 0.609          | 0.61           | 0.619        |
| CG Mus, bcf          | 0.758          | 0.775          | 0.914        |
| CG Per, bcf          | 0.25           | 0.254          | 0.281        |
| CG Soho, bcf         | 0.348          | 0.356          | 0.419        |
| CG Trot24, bcf       | 0.509          | 0.515          | 0.562        |
| CG Trot25, bcf       | 0.645          | 0.656          | 0.745        |
| CG Vre, bcf          | 0.663          | 0.678          | 0.786        |
| CG Zim, bcf          | 0.523          | 0.531          | 0.598        |
| <b>Total CG, bcf</b> | <b>4.858</b>   | <b>4.934</b>   | <b>5.528</b> |
| <b>Loss CG, bcf</b>  | <b>0.67</b>    | <b>0.594</b>   |              |

B.

|                          | ff9          | ff5          |
|--------------------------|--------------|--------------|
| Flwr, bcf                | 0.626        | 0.544        |
| Sec 23, bcf              | 0.527        | 0.461        |
| Sec 24, bcf              | 0.583        | 0.514        |
| Sec 26, bcf              | 0.803        | 0.712        |
| Sec 30, bcf              | 0.86         | 0.763        |
| Sec 31, bcf              | 0.669        | 0.582        |
| Sec 36, bcf              | 0.569        | 0.507        |
| <b>Total Infill, bcf</b> | <b>4.637</b> | <b>4.083</b> |

C.

|                             | ff9          | ff5          |
|-----------------------------|--------------|--------------|
| Loss CH P & CG, bcf         | 1.088        | 0.961        |
| Infill Prod, bcf            | 4.637        | 4.083        |
| <b>Incremental Rec, bcf</b> | <b>3.549</b> | <b>3.122</b> |

D.

Figure 18. A) Summary of simulator-calculated cumulative production (from 2008 to 2018) from existing Chase Parent wells with and without six vertical infill wells located such that each section in the Flower area had four producing wells. B) Summary of simulator-calculated cumulative production (from 2008 to 2018) from existing Council Grove wells with and without 6 vertical infill wells located such that each section in the Flower area had four producing wells. C) Summary of simulator-calculated cumulative production from vertical infills wells located such that each section has four producing wells. D) Summary of incremental gas recovery over 20 years due to drilling of six infill vertical wells. The hydraulic fractures at the infill wells were modeled using the ff-factor = 5 (to approximate  $H_f = 162$  ft and  $K_f = 11,000$  md) and ff-factor = 9 (to approximate  $H_f = 325$  ft and  $K_f = 11,000$  md).

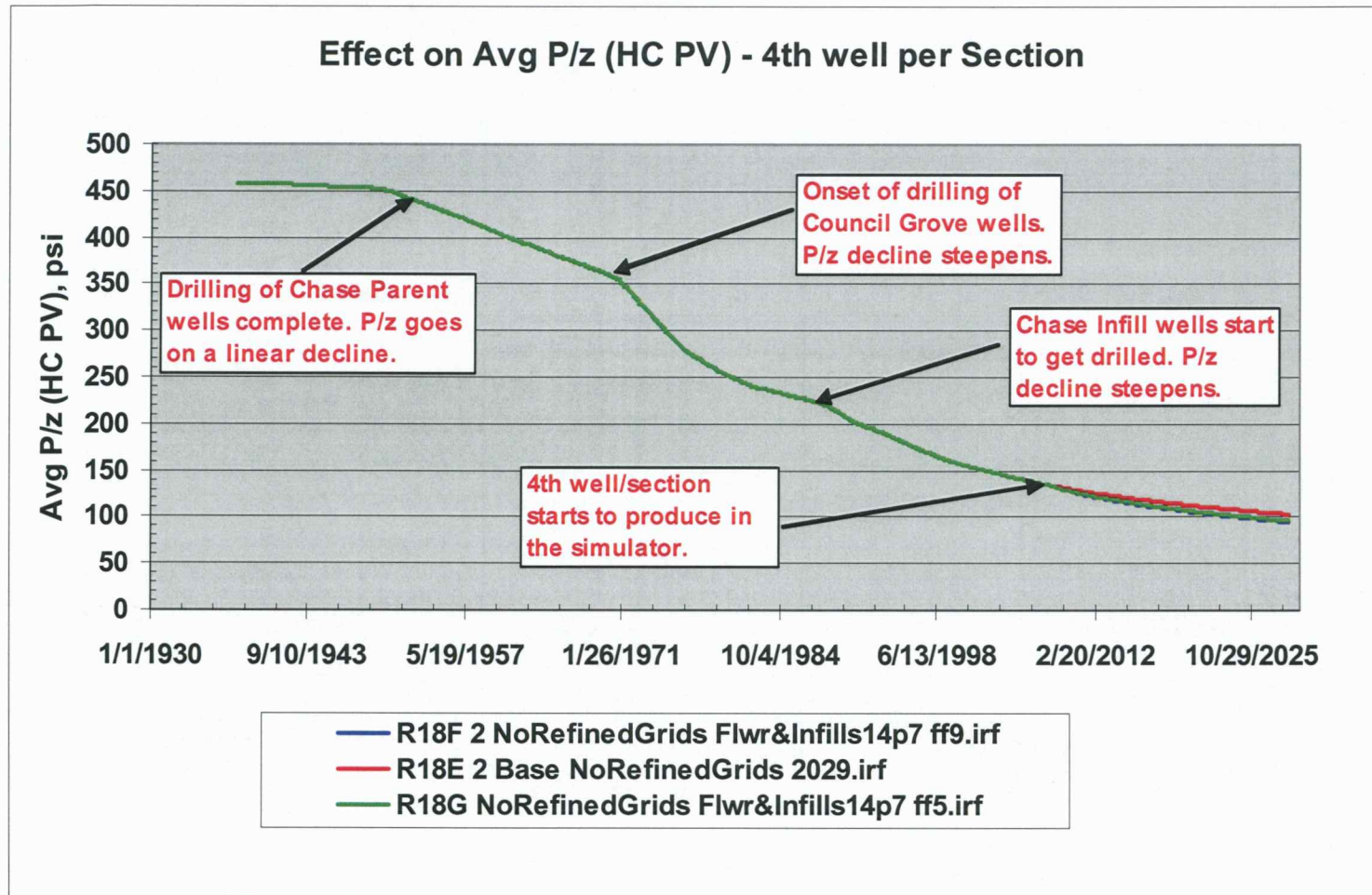


Figure 19. Plot of P/z averaged over hydrocarbon pore volume in the nine section area around the Flower A1 well over time assuming a) no infill drilling (curve in red), b) drilling of seven vertical infill wells and each modeled using ff-factor = 5 (to approximate  $H_f = 162$  ft and  $K_f = 11,000$  md and shown by the green curve), and c) drilling of seven vertical infill wells and each modeled using ff-factor = 9 (to approximate  $H_f = 325$  ft and  $K_f = 11,000$  md and shown by the green curve). The infill wells were located such that each of the sections in the Flower area had four producing wells.

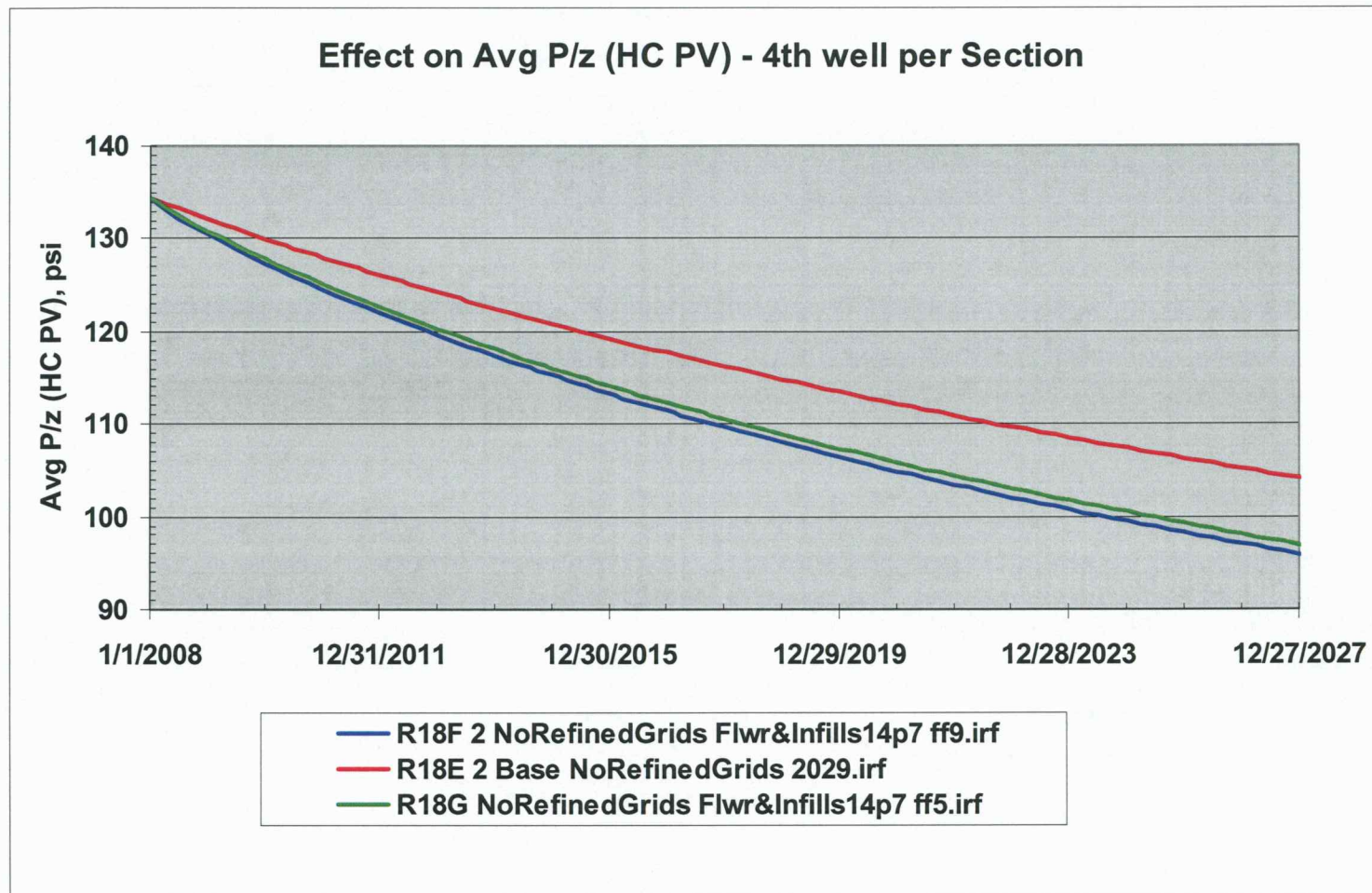


Figure 20. Hydrocarbon pore volume averaged P/z plot over the Flower area from 2008 to 2018 to show the effects of drilling seven vertical infill wells as of January 1, 2008. The curve in red is the base case where production comes from existing wells only, i.e., with no infill wells, while that in green represents the case where the infill fractures are modeled using  $ff = 5$  (to approximate  $H_f = 162$  ft and  $K_f = 11,000$  md). The curve in blue represents the case where the infill fractures are modeled using  $ff = 9$  (to approximate  $H_f = 325$  ft and  $K_f = 11,000$  md).